Corrosion behavior of anodized and Cathodic plasma electrolytic oxidation (CPEO) coatings on stainless steel used in nuclear spent fuel dry storage canister

Jun Heo [a], Jaewoo Lee [a], Sung Oh Cho [a*]
[a] Department of Nuclear and Quantum Engineering, Korea Advanced Institute of Science and Technology (KAIST), Daejeon 34141, Korea
[*]Corresponding author: socho@kaist.ac.kr

1. Introduction

Nuclear spent fuel storage is one of the most significant problem spotlighted nowadays in nuclear industry due to its safety issues resulting from radioactivity [1]. Spent fuel storage system is largely classified into two methods; wet and dry process. Usually wet storage system is adopted due to its advantages of easier access to the fuel for detection of issues and being flexible approach. However, it has been reported that, in Republic of Korea (ROK), wet storage of nuclear spent fuel is over-saturated. Alternatively, nuclear spent fuel dry storage adoptions are under consideration, focusing on advanced cases of overseas.

Dry storage system utilizes convection of air to cool the heat released from spent nuclear fuels. Dry storage systems are generally situated near the nuclear power plants which are located at the coastal region. High salinity and high humidity provided by the sea environment offer high corrosive environment to the materials used for dry storage system. Austenitic stainless steel (ASS), which is a material used for spent nuclear fuel containing canister, suffers various corrosion under the harsh environment of the seacoast. With welding process assisted, even more corrosion attacks will be served.

In order to enhance the durability of the metals, various coating technologies are developed [2-4]. Among them, electrochemical anodization and cathodic plasma electrolytic oxidation (CPEO) are in the limelight for stainless steel (SS) corrosion protection [5,6]. Anodization and CPEO stand for similar concept of applying voltage to the metal in a certain electrolyte. As a result, metal oxide layer is fabricated in both ways. However, their reactions on the surface and morphologies differ with each method.

In this study, comparison of the fabricated oxide layer on the metal surface through two different methods will be discussed. Surface morphologies, fabricated oxide layer depth, and finally their corrosion resistance properties are the main points of this research. By measuring their variety of characteristics, more effective coating method to improve the corrosion resistance of the SS will be identified.

2. Methods and Results

2.1 Materials and Characterization

Type 304 ASS used in CPEO and anodization was composed of 18-20 wt.% Cr, 8-10.5 wt.% Ni, <2 wt.% Mn and the remaining Fe (Goodfellow, UK). For CPEO, reagent grade sodium tetraborate decahydrate ($Na_2B_4O_7 \cdot 10H_2O$, borax, Sigma Aldrich, USA) and glycerol (Junsei Chemical, Japan) were used. For anodization, ethylene glycol (REAGENTPLUS, ≥99%, Sigma Aldrich, USA) and ammonium fluoride (NH_4F, Sigma Aldrich, USA) were used.

The morphology characterization of the specimen was conducted using a field emission scanning electron microscope (FESEM, Hitachi SU5000, Japan). The crystalline structure and composition of the specimen were examined using X-ray diffractometer (XRD, D/MAX 2500 V, Rigaku, Japan). An SP-200 Potentiostat/Galvanostat (Biologic, France) equipment was employed to perform electrochemical corrosion test.

2.2 Cathodic Plasma Electrolyte Oxidation (CPEO) & Anodization

CPEO was conducted with two-electrode system, which used SS specimen and SS container as working and counter electrode respectively (Figure 1a). In advance to CPEO, SS specimen was sonicated with acetone, ethanol, and deionized water for 5 min. each, followed by drying in vacuum oven. CPEO was, then, conducted at a unipolar direct current with potential of -180 V in an electrolyte containing 10 wt.% borax and 15 wt.% glycerol. The negative potential applied was adopted above the breakdown potential of SS, which is about 110 V. Initial voltage increase rate was 1 V/s and constant for 10 min. The duty cycle was maintained at 45% for negative potential and the frequency was kept with 100 Hz. After conducting CPEO, specimen was immersed in ethanol for 10 min. and stored in vacuum oven at 50 ℃.

In case of anodization, it also adopted two-electrode system in opposite position of target metal and counter electrode; SS as an anode and platinum sheet as a cathode. Pretreatment of the specimen was identical with the CPEO. Anodization was performed in an ethylene glycol-based electrolyte containing 0.1 M of NH_4F and 0.1 M of H_2O. Anodization was performed at a constant voltage of 60 V at 298 K for 7 min. After conducting anodization, specimen was also immersed in ethanol for 10 min. and stored in vacuum oven at 50 ℃.

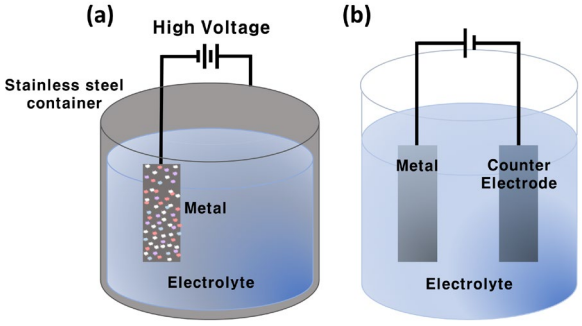

Figure 1. Schematic view of anodization and CPEO system

2.3 Morphology and Composition

When high voltage is applied to the metal in an electrolyte, the aqueous solution surrounding the metal is heated to form a gas envelope. With voltage over a critical value, breakdown of gas envelope results in plasma discharge on the metal surface. Then, according to extremely high temperature, active oxygen in the gas discharge envelope instantly reacts with the metal to form an oxide layer. Figure 2a shows the typical surface morphology of CPEO coatings on type 304 SS. The surface of the CPEO coatings is rough along with many fine particles, pores, and cracks. The pores are the specific regions that experienced high energy of the plasma discharges. CPEO is a repetitive surface deformation of oxidation and dissolution due to plasma cooling and heating. From those continuous actions, heterogeneous surface is formed such as cracks or covering layers. As depicted in Figure 2b, none of the cracks or pores penetrate through the oxide layer deep enough to reach the substrate. It refers that, cracks and pores on the oxide layer do not deteriorate the physical stability of the fabricated oxide layer. If the pores or cracks were deep enough to reach the substrate, corrosion or physical attacks from aggressive environment would be accelerated. Interesting phenomenon of the CPEO coating is that, the oxide layer growth heads both the inner and outer direction. As shown in Figure 2b, compact inner oxide layer and porous outer oxide layer is fabricated. Measured thickness of the CPEO coating oxide layer was approximately 22.3 μm. Uniform bonding of the dense inner layer with the substrate provides high adhesive strength of the fabricated oxide layer.

Anodization process uses much less voltage to form the oxide layer on the surface. With uniform voltage, electrochemical reactions in the electrolyte generates oxidation and dissolution process. In this process, dissolution is an etching phenomenon of fluorine compounds. Those etching reactions are controlled with electrolyte composition, temperature, and applying voltage to determine the nanostructure of the fabricated oxide layer. As shown in Figure 2c, uniformly distributed nanoporous oxide layer is formed on the metal surface. Average diameter of the fabricated nanopores were about 52 nm. Unlike CPEO coating, cracks or particles are hardly observable. This finding may result from uniform and stable chemical reaction during anodization compared to powerful impact of plasma discharge. From anodization, about 1.14 μm thick nanoporous oxide layer was fabricated. The role of nanopores along the oxide layer is to relieve the volume expansion stress. Oxide layer with general oxidation process brings accompanies cracks on the oxide layer surface, resulting in unstable protective layer. However, with anodization process, nanopores are generated with dissolution reactions, involving the stable and uniform oxide layer without cracks.

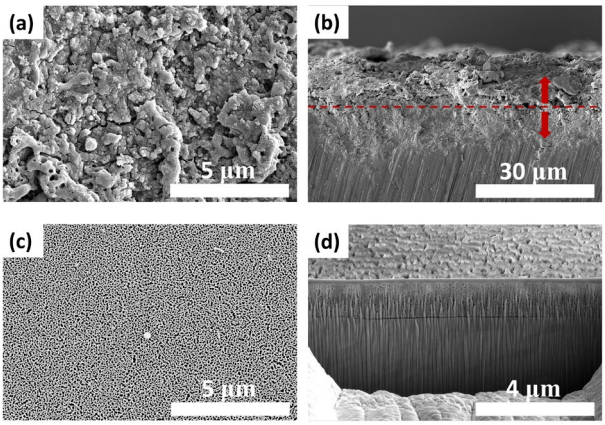

Figure 2. Surface and cross sectional FESEM images of (a,b)CPEO coated stainless steel and (c,d) anodized stainless steel

With XRD characterization, composition of the specimen was examined (Figure 3). Type 304 SS is mainly composed of austenitic iron, which is face centered cubic structure. After anodization, few different peaks were characterized with a substrate peak of austenite SS as a underlying composition. However, other peaks were substantially amorphous to be matched with noted peaks. It can be demonstrated that non-crystalline structure of the fabricated nanoporous oxide layer was responsible for those amorphous peaks with sharp austenite peaks from the substrate. Compared to the anodization specimen, CPEO sample showed additional peaks that were matched to the peaks of magnetite (Fe_3O_4). Austenite peaks were also characterized in this sample, with decreased peak intensities than anodized specimen. Those intensity drops might be resulted from thick oxide layer by CPEO process which can be an obstacle to detect the substrate composition. Relatively strong magnetite peaks refer to the formation of chemically stable oxide layer. With anodization process, it is known that heat treatment should be conducted to stabilize and crystallize the oxide layer formed on the surface. After the heat treatment of anodized sample, amorphous oxide layer

becomes crystalline structure with increased stability. However, with CPEO, heat treatment step can be skipped to fabricate protective oxide layer. Along with these compositional analysis, physical structure of the fabricated oxide layer, mentioned above, should be considered to evaluate the corrosion resisting behavior of the test specimen.

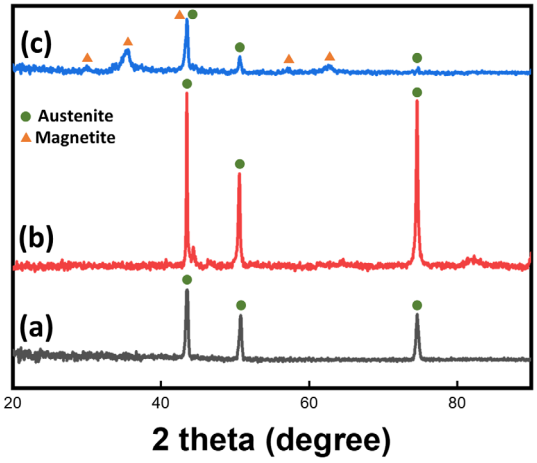

Figure 3. XRD spectra of (a) bare stainless steel, (b) anodized stainless steel, and (c) CPEO coated stainless steel

2.4 Potentiodynamic polarization technique

For the potentiodynamic polarization (PDP) test, conventional three electrode cell system was adopted. Samples with the exposed area of about 0.2 cm^2 were used as the working electrode, a platinum wire was used as the counter electrode, and a saturated calomel electrode was used for the reference electrode. PDP test was conducted to evaluate and compare the corrosion resisting behaviors of the test samples; bare SS, anodized SS, and CPEO coated SS. Before conducting PDP test, open circuit potential (OCP) was achieved by maintaining the samples in the electrode for 1200 sec. The potential range applied was ± 600 mV (vs. OCP). Lastly, the scan rate was 0.333 mV/s.

By extrapolating the anodic and cathodic tafel plots, corrosion potential (E_{corr}) and corrosion current (i_{corr}) can be obtained. Each parameter implies the meaning o f probability of corrosion and severity of corrosion, respectively. Corrosion rate can be calculated using i_{corr} value with below stated formula (1).

$$\mathrm{CR}(\mathrm{mm\ year^{-1}}) = \frac{i_{corr}(Acm^{-2}) \times M(g)}{n \times d(gcm^{-3}) \times A(cm^2)} \times 3272 \quad (1)$$

All the parameters measured are tabulated in table 1. We can easily figure out the down-rightward movements of the PDP curves after treatment with simple inspection (Figure 4). Those movements imply that increase in E_{corr} value and decrease in i_{corr} value of the electrochemically treated samples. As shown in table 1, bare SS, anodized SS, and CPEO coated SS exhibits E_{corr} value of -319.2, -222.0, and -125.5 mV/SCE, respectively. It can be interpreted that the probabilities of the samples were improved due to electrochemical treatment. Among two treated samples, CPEO coated sample showed more higher value of E_{corr}, meaning less chance of corrosion attack. Perhaps, due to chemical stability of the fabricated magnetite (Fe_3O_4) oxide layer with CPEO process, CPEO samples showed improved corrosion probability value. Anodized sample also showed improved Ecorr value than bare SS. Nanoporous oxide layer formed on the surface of the SS is expecting to be acted as a protective barrier against the corrosion attack. In respect of icorr, interestingly, anodized sample showed lower value than any other samples, which means the improvement of corrosion resistance in terms of severity. Anodized and CPEO coated samples showed relatively small difference in i_{corr} value. Lower i_{corr} value of the anodized sample might be explained using uniform nanoporous oxide layer structure. As we can observe from the Figure 2 images, oxide layer fabricated by anodization perfectly blocks the access of outer corrosive substances. In case of CPEO coated sample, due to thick oxide layer, cracks are formed resulting from volume expansion stress. Those cracks leave a choice for the outer corrosive materials to penetrate to the substrate resulting in corrosion attack. As tabulated in table 1, corrosion rate can be calculated as followings; 1.973×10^{-2} mm/yr for bare SS, 6.124×10^{-3} mm/yr for anodized SS, and 7.084×10^{-3} mm/yr for CPEO coated SS. Anodized sample exhibited lowest value of corrosion rate with no doubt, owing to lowest i_{corr} value.

Table 1. Potentiodynamic polarization test parameters

Type	E_{corr} (mV/SCE)	i_{corr} (A/cm^2)	CR (mm/yr)
Bare SS	-319.2	1.83×10^{-6}	1.973×10^{-2}
Anodized SS	-222.0	5.68×10^{-7}	6.124×10^{-3}
CPEO coated SS	-125.5	6.57×10^{-7}	7.084×10^{-3}

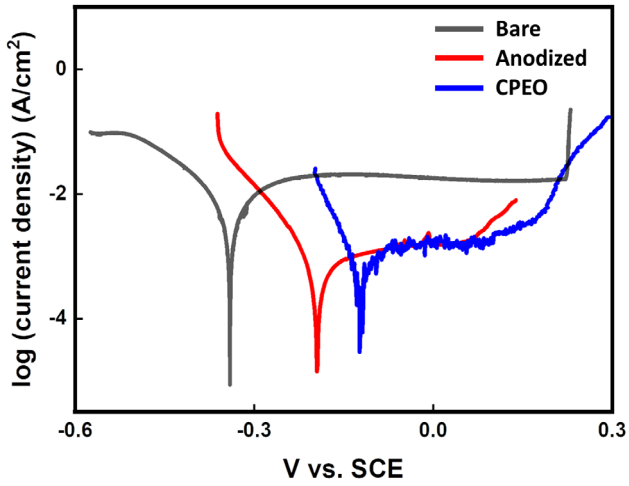

Figure 4. Potentiodynamic polarization curves of bare, anodized, and CPEO coated stainless steel

3. Conclusions

In this study, corrosion behavior of the anodized and CPEO coated SS has been discussed utilizing the physical morphology inspection and electrochemical test. Using FESEM characterization, surface morphology and thickness of the fabricated oxide layer were measured. In case of CPEO coated SS, relatively thick oxide layer with approximately 22.3 um was grown in both outward and inward. The surface was irregular with pores, cracks, and covering layers, perhaps, due to high energy reactions with plasma discharge. With anodized sample, uniform nanoporous oxide layer was inspected on the surface with approximately 52 nm pores. In cross sectional view, a clear distinction was characterized between the substrate and the oxide layer with constant thickness of 1.14 um. Both the surface and cross-sectional morphologies were highly uniform with anodized sample compared to CPEO coated sample. Relatively steady reaction compared to explosive reactions of CPEO would be the possible reason for those uniform morphologies. To compare the corrosion resisting properties of the bare SS, anodized SS, and CPEO coated SS, electrochemical test was conducted. Through PDP test, E_{corr}, i_{corr}, and corrosion rates were calculated. In E_{corr} point of view, CPEO coated SS showed most improved behavior compared to anodized sample. However, in i_{corr} and corrosion rate point of view, anodized sample was slightly superior. Summarizing the results from this research, CPEO coated and anodized samples had both advantages and disadvantages. For CPEO coated sample, better adhesion of oxide layer, stable composition of magnetite, and resulted higher value of E_{corr} was characterized. In opposite, it showed lots of cracks on the oxide layer resulting in poor i_{corr} and corrosion rate value than anodized sample. In case of anodized sample, although it showed less adhesive property of the oxide layer and lower value of E_{corr}, higher uniformity of the fabricated oxide layer was achieved resulting in improved corrosion rate with better i_{corr} value than CPEO coated sample. It can be concluded that corrosion resistance improving technology should be selected compromising the gains and loss.

REFERENCES

[1] Saegusa, T., Shirai, K., Arai, T., Tani, J., Takeda, H., Wataru, M., ... & Winston, P. L. (2010). Review and future issues on spent nuclear fuel storage. Nuclear Engineering and Technology, 42(3), 237-248.

[2] Raman, R. S., Banerjee, P. C., Lobo, D. E., Gullapalli, H., Sumandasa, M., Kumar, A., ... & Majumder, M. (2012). Protecting copper from electrochemical degradation by graphene coating. Carbon, 50(11), 4040-4045.

[3] Xue, D., Yun, Y., Schulz, M. J., & Shanov, V. (2011). Corrosion protection of biodegradable magnesium implants using anodization. Materials Science and Engineering: C, 31(2), 215-223.

[4] Lao, L., Liu, K., Ren, L., Yu, J., Cheng, J., Li, Y., & Lu, S. (2021). Improving Corrosion Protection and Friction Resistance of Q235 Steel by Combining Noncovalent Action and Rotating Coating Method. ACS Omega.

[5] Bouchama, L., Azzouz, N., Boukmouche, N., Chopart, J. P., Daltin, A. L., & Bouznit, Y. (2013). Enhancing aluminum corrosion resistance by two-step anodizing process. Surface and Coatings Technology, 235, 676-684.

[6] Wu, J., Zhang, Y., Liu, R., Wang, B., Hua, M., & Xue, W. (2015). Anti-corrosion layer prepared by plasma electrolytic carbonitriding on pure aluminum. Applied Surface Science, 347, 673-678.